Impact ionization in balance equation theory

1995 J. Phys.: Condens. Matter 7 7871

(http://iopscience.iop.org/0953-8984/7/40/017)

J. Phys.: Condens. Matter 7 (1995) 7871–7878. Printed in the UK

Impact ionization in balance equation theory

X F Wang and X L Lei

China Centre of Advanced Science and Technology (World Laboratory), PO Box 8730, Beijing 100080, People's Republic of China
Shanghai Institute of Metallurgy, Chinese Academy of Sciences, 865 Changning Road, Shanghai 200050, People's Republic of China

Received 23 May 1995, in final form 17 July 1995

Abstract. We present a theoretical investigation of electron impact ionization processes under a high electric field within the framework of the Lei–Ting balance equation approach in the case where the hole gas is approximately in thermal equilibrium. An expression for the impact ionization coefficient for an arbitrary conduction band is obtained. As an example, the impact ionization coefficient of bulk InSb is calculated in the approximation of a parabolic conduction band and the result is compared with existing experimental data.

1. Introduction

High-field-induced hot carriers have made impact ionization (II) a very important process in modern semiconductor devices. Although a hindrance resulting in device breakdown and degradation, II has also been widely exploited in electronic devices such as semiconductor lasers and charge multiplication devices. As a result, many authors have devoted great effort to theories describing the impact ionization process [1–25]. Based on the early theory of the electrical ionization coefficient by Wolff [1], Shockley [2] and Baraff [3], a semiclassical lucky-drift theory was developed by Ridley [4], and was later improved by Burt [5] and Wilson [6], to describe impact ionization in moderate-to-large-energy-gap semiconductors. Dumke [7] has constructed a theory of avalanche breakdown for narrow-gap semiconductors such as InSb and InAs, in which the primary electron-scattering mechanism is polar-optical-mode scattering. Recently, a more rigorous analytical expression within the hydrodynamic approach was employed by Quade and co-workers [8] to study II in semiconductor high-field transport. Goldsman [9, 10] has presented a method for calculating II coefficients by solving the Boltzmann equation. Wang and co-workers [11, 12] have used an ensemble Monte Carlo simulation to calculate II coefficients in Si and GaAs including a wavevector-dependent numerical transition rate formulation, which goes beyond the limitation of the Keldysh formula [13] used in early Monte Carlo calculations. A Monte Carlo simulation including full band structure and an anisotropic impact ionization model was also carried out by Kunikiyo and co-workers [14] to estimate the II coefficient in Si. Integrating the Boltzmann transport equation by the Monte Carlo method, Arnold and co-workers [15] studied the II-related transport phenomena in silicon dioxide. Furthermore, Quade and co-workers [16] applied a quantum-mechanical approach based on the density-matrix formalism with the inclusion of distribution functions and the Pauli exclusion principle to study impact ionization, but they did not compare their theoretical result with experiment.

Over the past several years, the Lei–Ting balance equation theory [26] and its extension [27] have been widely used to study high-field transport in semiconductors.

0953-8984/95/407871+08$19.50

So far II has been excluded from the theory. In this paper, we present an analytical theory describing impact ionization processes in high electric fields within the framework of the Lei–Ting balance equation theory in terms of non-equilibrium Green functions. As a simple example, we examine energy and momentum relaxation and the electron–hole pair generation rate due to impact ionization in bulk InSb.

2. Theory

We consider the transport of a uniform n-type semiconductor in an electric field $\boldsymbol{E}$. If the effective hole mass m_h^* is much larger than the effective electron mass m_e^*, the drift movement and heating of hole gases are negligible in comparison with those of the electron gases, so we can treat the hole gases as motionless with a lattice temperature T. The Hamiltonian of the system is ($\hbar = 1 = k_B$ throughout the paper)

$$H = H_E + H_e + H_{ph} + H_h + H_{ei} + H_{e-ph} + H_{ii}. \tag{1}$$

Here, H_E, H_e, H_{ph}, H_{ei} and H_{e-ph} are respectively the uniform electric field potential, the electron Hamiltonian, the phonon Hamiltonian, electron–impurity and electron–phonon interactions as mentioned in [26, 27].

To take account of the impact ionization process, we have added H_h, the Hamiltonian of hole gases, and H_{ii}, the Hamiltonian of the band–band impact ionization process in (1). For an incident electron of a given spin, there are two types of indistinguishable and two types of distinguishable II process [28]. The two types of indistinguishable II process, where the collision particles have identical spins, interfere with each other and their total contribution to transition rate is negligible. As an approximation, we neglect the indistinguishable II processes in H_{ii}, and interaction between particles in H_e and H_h. We have

$$H_e = \sum_{k,\sigma} \varepsilon_k C_{k,\sigma}^\dagger C_{k,\sigma} \tag{2}$$

$$H_h = \sum_{k,\sigma} \varepsilon_k^h d_{k,\sigma}^\dagger d_{k,\sigma} \tag{3}$$

$$H_{ii} = \sum_{k,k'q,\sigma} M_q^{ii} C_{k+q,\bar{\sigma}}^\dagger C_{k-q,\sigma}^\dagger d_{-k,\sigma}^\dagger C_{k',\bar{\sigma}} + M_{-q}^{ii} C_{k',\bar{\sigma}}^\dagger d_{-k,\sigma} C_{k-q,\sigma} C_{k'+q,\bar{\sigma}} \tag{4}$$

with $d_{k,\sigma}^\dagger$ ($d_{k,\sigma}$) being the creation (annihilation) operator of the hole, $C_{k,\sigma}^\dagger$ ($C_{k,\sigma}$) being the creation (annihilation) operator of the electron, and $\bar{\sigma}$ denoting the inverse spin of σ; M_q^{ii} is the Fourier representations of the band–band Coulomb interaction matrix element

$$M_q^{ii} = \frac{e^2}{\kappa \epsilon_0 (q^2 + q_0^2)} I_{cc} I_{cv} \tag{5}$$

with a constant dielectric screening κ, and a reciprocal screening length q_0. I_{cc} and I_{cv} are overlap integrals of conduction–conduction bands and conduction–valence bands respectively. Since $I_{cv} = 0$ when $q = 0$, we assume $M_0^{ii} = 0$ through out this paper.

The velocity operator of the centre-of-mass in the Lei–Ting balance equation theory is

$$\hat{\boldsymbol{v}} = -\mathrm{i}[\boldsymbol{R}, H] = \frac{1}{N_e} \sum_{k,\sigma} \boldsymbol{v}(k) C_{k,\sigma}^\dagger C_{k,\sigma} \tag{6}$$

where $v(k) = \nabla\varepsilon(k)$ is the velocity function.

The time derivatives of the centre-of-mass velocity $\hat{v}$, of the relative electron Hamiltonian H_e, and of the electron number $\hat{N}_e$, can be derived as follows:

$$\begin{aligned}\frac{\mathrm{d}(N_e\hat{v})}{\mathrm{d}t} &= N_e eE\cdot\hat{\mathcal{K}} - \mathrm{i}\sum_{q,a}U(q)\mathrm{e}^{\mathrm{i}q\cdot R_a}\sum_{k,\sigma}[v(k+q)-v(k)]C^{\dagger}_{k+q,\sigma}C_{k,\sigma}\\ &\quad -\mathrm{i}\sum_{q,\lambda}M(q,\lambda)(b_{q,\lambda}+b^{\dagger}_{-q,\lambda})\sum_{k,\sigma}[v(k+q)-v(k)]C^{\dagger}_{k+q,\sigma}C_{k,\sigma}\\ &\quad -\mathrm{i}\sum_{k,k'q,\sigma}[v(k-q)+v(k'+q)-v(k')]M^{ii}_{q}C^{\dagger}_{k-q,\bar{\sigma}}d^{\dagger}_{-k,\bar{\sigma}}C^{\dagger}_{k'+q,\sigma}C_{k',\sigma}\\ &\quad -\mathrm{i}\sum_{k,k'q,\sigma}[v(k')-v(k-q)-v(k'+q)]M^{ii}_{-q}d_{-k,\bar{\sigma}}C_{k-q,\bar{\sigma}}C^{\dagger}_{k',\sigma}C_{k'+q,\sigma}\end{aligned}\tag{7}$$

$$\begin{aligned}\dot{H}_e = -\mathrm{i}[H_e,H] &= -\mathrm{i}\Big[\sum_{k,\sigma}\varepsilon_k C^{\dagger}_{k,\sigma}C_{k,\sigma},H\Big]\\ &= N_e eE\cdot\hat{v} - \mathrm{i}\sum_{q,a}U(q)\mathrm{e}^{\mathrm{i}q\cdot R_a}\sum_{k,\sigma}(\varepsilon_{k+q}-\varepsilon_k)C^{\dagger}_{k+q,\sigma}C_{k,\sigma}\\ &\quad -\mathrm{i}\sum_{q,\lambda}M(q,\lambda)(b_{q,\lambda}+b^{\dagger}_{-q,\lambda})\sum_{k,\sigma}(\varepsilon_{k+q}-\varepsilon_k)C^{\dagger}_{k+q,\sigma}C_{k,\sigma}\\ &\quad -\mathrm{i}\sum_{k,k'q,\sigma}(\varepsilon_{k-q}+\varepsilon_{k'+q}-\varepsilon_{k'})M^{ii}_{q}C^{\dagger}_{k-q,\bar{\sigma}}d^{\dagger}_{-k,\bar{\sigma}}C^{\dagger}_{k'+q,\sigma}C_{k',\sigma}\\ &\quad -\mathrm{i}\sum_{k,k'q,\sigma}(\varepsilon_{k'}-\varepsilon_{k-q}-\varepsilon_{k'+q})M^{ii}_{-q}d_{-k,\bar{\sigma}}C_{k-q,\bar{\sigma}}C^{\dagger}_{k',\sigma}C_{k'+q,\sigma}\end{aligned}\tag{8}$$

$$\begin{aligned}\dot{N}_e &= -\mathrm{i}[\hat{N}_e,H]\\ &= -\mathrm{i}\sum_{k,k'q,\sigma}[M^{ii}_{q}C^{\dagger}_{k-q,\bar{\sigma}}d^{\dagger}_{-k,\bar{\sigma}}C^{\dagger}_{k'+q,\sigma}C_{k',\sigma} - M^{ii}_{-q}d_{-k,\bar{\sigma}}C_{k-q,\bar{\sigma}}C^{\dagger}_{k',\sigma}C_{k'+q,\sigma}].\end{aligned}\tag{9}$$

Following balance transport theory [17, 26] to the approximation that the hole gas is in thermal equilibrium with the lattice temperature T, we define the interaction picture for an operator $\hat{O}$ as

$$\hat{O}(t) = \exp[\mathrm{i}(H_e+H_E+H_{ph}+H_h)t]\hat{O}\exp[-\mathrm{i}(H_e+H_E+H_{ph}+H_h)t]\tag{10}$$

and derive the density matrix in the interaction picture from the integral equation

$$\hat{\rho}(t) = \hat{\rho}_0 - \mathrm{i}\int_0^t \mathrm{d}t_1[H_I(t_1),\hat{\rho}(t_1)]\tag{11}$$

where $\hat{\rho}_0$ is the initial density matrix and $H_I = H_{ei}+H_{e-ph}+H_{it}$ stands for the interaction Hamiltonian.

The initial density matrix ρ_0 takes the form

$$\rho_0 = \exp[-(H_{er}-\mu_e\hat{N}_e)/T_e]|P_d\rangle\langle P_d|\exp[-(H_h-\mu_h\hat{N}_h)/T]\exp(-H_{ph}/T).\tag{12}$$

Here $P_d = N_e p_d$ is the total momentum of the electron system and H_{er} represents the relative electron Hamiltonian

$$H_{er} = \sum_{k,\sigma} \varepsilon(k - p_d) C^{\dagger}_{k\sigma} C_{k\sigma} = \sum_{k,\sigma} \bar{\varepsilon}(k) C^{\dagger}_{k\sigma} C_{k\sigma}.$$

Taking the statistical average of the operator equations (7)–(9) with respect to the lowest-order density matrix, we obtain the time derivative of the electron drift velocity and the average electron energy:

$$\frac{\mathrm{d}v_d}{\mathrm{d}t} = \left\langle \frac{\mathrm{d}\hat{v}}{\mathrm{d}t} \right\rangle = eE \cdot \mathcal{K} + A_{ei} + A_{ep} + A_{ii} - \frac{1}{N_e}\frac{\mathrm{d}N_e}{\mathrm{d}t} v_d \tag{13}$$

$$\frac{\mathrm{d}h_e}{\mathrm{d}t} = eE \cdot v_d - W_{ep} - W_{ii} - \frac{1}{N_e}\frac{\mathrm{d}N_e}{\mathrm{d}t} h_e \tag{14}$$

and the electron–hole generation rate ($g \equiv \mathrm{d}N_e / N_e \,\mathrm{d}t$)

$$\begin{aligned} g = \langle \dot{N}_e \rangle / N_e = \frac{4\pi}{N_e} \sum_{k,k',q} |M^{ii}_q|^2 \delta(\varepsilon_{k-q} + \varepsilon^h_k + \varepsilon_{k'+q} - \varepsilon_{k'}) f\left(\frac{\bar{\varepsilon}_{k'} - \mu}{T_e}\right) \\ \times \left[1 - f\left(\frac{\bar{\varepsilon}_{k'+q} - \mu}{T_e}\right)\right]\left[1 - f\left(\frac{\bar{\varepsilon}_{k-q} - \mu}{T_e}\right)\right] \\ \times \left(1 - \frac{f[(\varepsilon^h_k - \mu^h)/T]}{f[(\bar{\varepsilon}_{k'} - \bar{\varepsilon}_{k-q} - \bar{\varepsilon}_{k'+q} + \mu)/T_e]}\right). \end{aligned} \tag{15}$$

Here A_{ii} is the frictional acceleration due to impact ionization:

$$\begin{aligned} A_{ii} = \frac{4\pi}{N_e} \sum_{k,k',q} |M^{ii}_q|^2 \delta(\varepsilon_{k-q} + \varepsilon^h_k + \varepsilon_{k'+q} - \varepsilon_{k'}) [v(k'+q) + v(k-q) - v(k')] f\left(\frac{\bar{\varepsilon}_{k'} - \mu}{T_e}\right) \\ \times \left[1 - f\left(\frac{\bar{\varepsilon}_{k'+q} - \mu}{T_e}\right)\right]\left[1 - f\left(\frac{\bar{\varepsilon}_{k-q} - \mu}{T_e}\right)\right] \\ \times \left(1 - \frac{f[(\varepsilon^h_k - \mu^h)/T]}{f[(\bar{\varepsilon}_{k'} - \bar{\varepsilon}_{k-q} - \bar{\varepsilon}_{k'+q} + \mu)/T_e]}\right) \end{aligned} \tag{16}$$

and W_{ii} is the energy loss rate due to impact ionization:

$$\begin{aligned} W_{ii} = \frac{4\pi}{N_e} \sum_{k,k',q} |M^{ii}_q|^2 \varepsilon^h_k \delta(\varepsilon_{k-q} + \varepsilon^h_k + \varepsilon_{k'+q} - \varepsilon_{k'}) f\left(\frac{\bar{\varepsilon}_{k'} - \mu}{T_e}\right) \\ \times \left[1 - f\left(\frac{\bar{\varepsilon}_{k'+q} - \mu}{T_e}\right)\right]\left[1 - f\left(\frac{\bar{\varepsilon}_{k-q} - \mu}{T_e}\right)\right] \\ \times \left(1 - \frac{f[(\varepsilon^h_k - \mu^h)/T]}{f[(\bar{\varepsilon}_{k'} - \bar{\varepsilon}_{k-q} - \bar{\varepsilon}_{k'+q} + \mu)/T_e]}\right). \end{aligned} \tag{17}$$

The expression of frictional accelerations due to impurity (A_{ei}) and phonon (A_{ep}) scatterings, and the energy loss rate due to phonon scatterings (W_{ep}) can be found in [27], $h_e \equiv \langle H_e \rangle / N_e$ is the electron energy per carrier,

$$v_d = \frac{2}{N_e} \sum_k v(k) f[(\bar{\varepsilon}(k) - \mu)/T_e] \tag{18}$$

is the average drift velocity of electrons,

$$\mathcal{K} = \frac{2}{N_e}\sum_{k} \nabla\nabla\varepsilon(k) f[(\bar{\varepsilon}(k) - \mu)/T_e] \tag{19}$$

is the average inverse effective mass tensor, $f(x) = (e^x - 1)^{-1}$ is the Fermi function, μ (μ^h) is the electron (hole) chemical potential, and T_e is the electron temperature.

Electron–hole pair generation rates are usually measured experimentally when the electron drift velocity and electron temperature become steady, since in most materials the momentum and energy relaxation times are much shorter than the carrier-number relaxation time. This corresponds to the case where the left-hand sides of (13) and (14) equal zero. By solving those balance equations to determine the electron transport parameters T_e and p_d, we can evaluate theoretically the electron–hole pair generation rate g due to impact ionization and ionization coefficients $\alpha_n = g/v_d$ of electrons from (15).

3. Results

In the following, we discuss the electron impact ionization generation rate in InSb when an electron field is applied along the z direction. The energy band of InSb can be described by the Kane band formula

$$\varepsilon(1 + \alpha\varepsilon) = k^2/2m_c \tag{20}$$

where $\alpha = 1/E_g$ is the non-parabolic parameter; E_g is the energy gap and m_c is the electron band-edge effective mass. Then the velocity of an electron with momentum k is

$$v(k) = \nabla\varepsilon = k(m_c^2 + 2\alpha m_c k^2)^{-1/2} \tag{21}$$

and the diagonal component of the inverse effective mass tensor $\mathcal{K}_{zz}$ is

$$\mathcal{K}_{zz} = 1/m^* = \frac{2}{N_e}\sum_{k}\frac{\partial^2\varepsilon}{\partial k_z^2} f\left(\frac{\bar{\varepsilon}(k) - \mu}{T_e}\right) = \frac{2}{N_e}\sum_{k}\frac{1}{m_c}\frac{f[(\bar{\varepsilon}(k) - \mu)/T_e]}{(1 + 2\alpha k^2/m_c)^{3/2}}. \tag{22}$$

During the process of numerically calculating the electric field dependence of the impact ionization coefficient, we find that the result is very sensitive to the electric field dependence of the electron mobility and the average electron energy. In electric fields less than $400\,\mathrm{V\,cm^{-1}}$, before the avalanche breakdown begins to happen, the impact ionization process is an inferior scattering mechanism in comparison with the polar electron–phonon interaction in InSb. Therefore we have used the exact Kane band to evaluate A_{ei}, A_{ep} and W_{ep}, which mainly determine the electron transport properties, but for the sake of simplicity used an approximately parabolic band with an electric-field-dependent average effective electron mass $m^* = 1/\mathcal{K}_{zz}$ to estimate the A_{ii}, W_{ii} and g ($\varepsilon(k) = k^2/2m^*$). In the parabolic band approximation, (15)–(17) become

$$g = \frac{4\pi}{N_e}\sum_{k,q}|M_q^{ii}|^2\sum_{k'} f\left(\frac{\xi_{k'}}{T_e}\right)\left[1 - f\left(\frac{\xi_{k-q}}{T_e}\right)\right]\left[1 - f\left(\frac{\xi_{k'+q}}{T_e}\right)\right]$$
$$\times\left(1 - \frac{f(\xi_k^h/T)}{f[\xi_{k'} - \xi_{k-q} - \xi_{k'+q})/T_e]}\right)\delta(\omega_1 + \tfrac{1}{2}m^* v_d^2 + \varepsilon_k^h + \varepsilon_{k'+q} + \varepsilon_{k+q} - \varepsilon_{k'})$$

$$= \frac{2}{N_e}\sum_{k,q}|M_q^{ii}|^2\Pi_2(q,\omega_2)\left[f\left(\frac{\xi_{k-q}}{T_e}\right)+n\left(\frac{\omega_2}{T_e}\right)\right]$$
$$\times\left[f\left(\frac{\xi_k^h}{T}\right)-f\left(\frac{\omega_1+m^*v_d^2/2+\varepsilon_k^h+\mu}{T_e}\right)\right] \tag{23}$$

$$A_{ii} = \frac{2}{m^*N_e}\sum_{k,q}|M_q^{ii}|^2k_z\Pi_2(q,\omega_2)\left[f\left(\frac{\xi_{k-q}}{T_e}\right)+n\left(\frac{\omega_2}{T_e}\right)\right]$$
$$\times\left[f\left(\frac{\xi_k^h}{T}\right)-f\left(\frac{\omega_1+m^*v_d^2/2+\varepsilon_k^h+\mu}{T_e}\right)\right] \tag{24}$$

$$W_{ii} = \frac{2}{N_e}\sum_{k,q}|M_q^{ii}|^2(\omega_1+\tfrac{1}{2}m^*v_d^2+\varepsilon_k^h)\Pi_2(q,\omega_2)$$
$$\times\left[f\left(\frac{\xi_{k-q}}{T_e}\right)+n\left(\frac{\omega_2}{T_e}\right)\right]\left[f\left(\frac{\xi_k^h}{T}\right)-f\left(\frac{\omega_1+m^*v_d^2/2+\varepsilon_k^h+\mu}{T_e}\right)\right]. \tag{25}$$

In the above equations, $\omega_0 = q_x v_d$, $\omega_1 = k_x v_d$, $\omega_2 = \omega_1 + m^*v_d^2/2 + \varepsilon_k^h + \varepsilon_{k-q}$, $\xi_k = \varepsilon_k - \mu$ is the energy of an electron with momentum k measured from the electron Fermi energy μ, and $\xi_k^h = \varepsilon_k^h - \mu^h$ is the energy of a hole with momentum k measured from the hole Fermi energy μ^h; $\Pi_2(q,\omega)$ represents the imaginary parts of electron–electron correlation functions and $n(x) \equiv (e^x - 1)^{-1}$ is the Bose function.

The parameters used in this paper for InSb are listed in table 1.

Table 1. Parameters for Insb.

Parameter	Unit	Value
Optical dielectric $\kappa_{1\infty}$	1	15.68
Low-frequency dielectric constant κ_{1s}	1	17.54
Effective electron edge-band mass m_e	m_e	0.0138
Effective hole mass m^*	m_e	0.4
Band gap	eV	0.225
Material density d	$\mathrm{g\,cm^{-3}}$	5.775
Longitudinal sound velocity v_{sl}	$\mathrm{m\,s^{-1}}$	3.75×10^3
Longitudinal optic phonon energy ω_{L1}	eV	2.42×10^{-2}
Acoustic deformation potential Ξ	eV	20

In the numerical calculation, we have employed the Thomas–Fermi screening in (6) to evaluate the inverse screening length and $q_0 = 6\pi N_e e^2/\mu$. The value of $I_{cc}I_{cv}/\kappa$ is assumed to be a constant and is determined by fitting the theoretical result to experimental data.

In figure 1, we compare the calculated electron drift mobility in InSb with the experimental result [29] when the electron density is $n_e = 1.8 \times 10^{14}\,\mathrm{cm^{-3}}$ and the linear mobility is $\mu_0 = 5.4 \times 10^5\,\mathrm{cm^2\,V^{-1}\,s^{-1}}$. Since we have only used a very simple static-screening Coulomb potential to describe the impurity scattering, the theoretical curve does not coincide with the experimental one completely. However, the calculated mobility agrees well with the experimental result in electric fields higher than $200\,\mathrm{V\,cm^{-1}}$ when impact ionization begins to contribute.

In figure 2, the corresponding electron–hole pair generation rate g in InSb is plotted against electric field E. The result fits a function of the form $g(E) \propto E^m$ with $m = 14$ for electric fields in the range 200–400 $\mathrm{V\,cm^{-1}}$. For the sake of comparison, the experimental

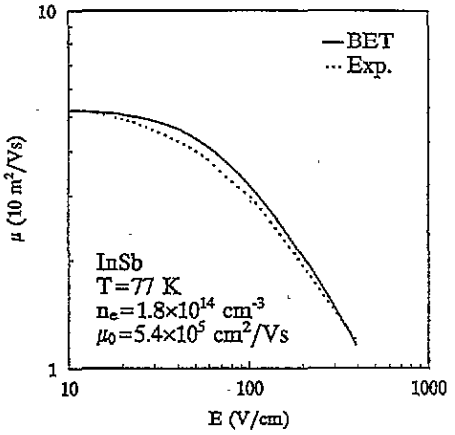

Figure 1. Electron mobility of InSb at a temperature $T = 77\,\mathrm{K}$ as a function of electric field when the electron density $n_e = 1.8 \times 10^{14}\,\mathrm{cm}^{-3}$. The full curve denotes the result of balance equation theory; the dotted curve is the experimental result from [29].

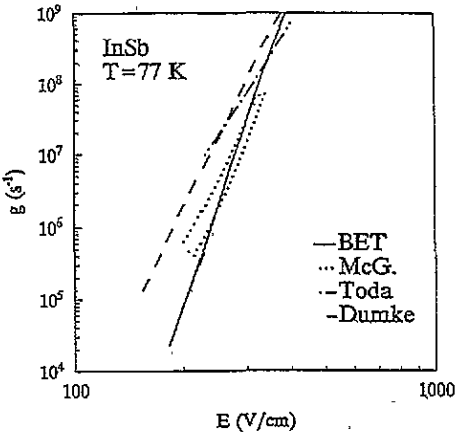

Figure 2. Comparison of electron-induced pair generation rate g of InSb from balance equation theory (full curve) with theoretical and experimental results in the literature.

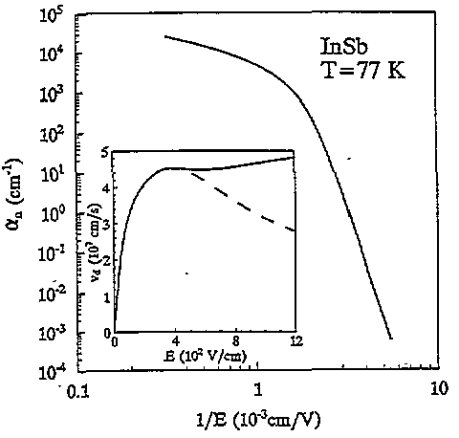

Figure 3. Calculated electron impact ionization coefficient α_n of InSb from balance equation theory as a function of inverse electric field (parameters are the same as in figures 1 and 2). In the inset, the calculated electron drift velocities including II processes (full curve) and without II processes (broken curve) are illustrated as a function of electric field.

results of McGroddy and Nathan [30] and Toda [31] are illustrated with the dotted and chain curves respectively. The result of McGroddy and Nathan fits a power law with $m = 10$, while Toda's result fits a power law with $m = 8$. Here we find that the calculated generation rate increases with electric field more quickly than do the experimental results. This deviation may stem from the parabolic conduction band approximation used when evaluating the electron–hole pair generation rate. The calculated result of Dumke [7] at temperature $T = 0\,\mathrm{K}$ is shown with the broken curve.

In figure 3 we plot the electron impact ionization coefficient α_n of InSb as a function of inverse electron field. Since the drift velocity of electrons in InSb under an electric field between 200–400 $\mathrm{V\,cm}^{-1}$ is nearly constant, α_n also shows a power law relation with electric field, as does the generation rate g. When the electric field is larger than 400 $\mathrm{V\,cm}^{-1}$, the scattering rate due to impact ionization becomes comparable to the polar optic phonon scattering rate. The rate of the ionization coefficient with electric field slows down as a

result of the high energy loss rate due to the II process. On the other hand, the calculated drift velocity including the II process (full curve) is higher than that without the II process (broken curve), as shown in the inset of figure 3, because the high-energy electrons are scattered to low-energy states by II processes similar to the case discussed in [20].

In conclusion, within the framework of the Lei–Ting balance equation theory, we have obtained a formula for calculating the electron impact ionization coefficient in a high electric field in the case where the hole gas stays approximately in thermal equilibrium. In the derivation, we have neglected the influence of the intraband Coulomb interaction on impact ionization. As a typical example, the electron impact ionization coefficient of bulk InSb is calculated by assuming constant overlap integration. We have used the Kane model to describe the conduction band in calculating impurity and phonon scattering rates, but employed the parabolic band approximation in carrying out the integration for impact ionization processes. The comparison between theoretical and experimental results was discussed.

References

[1] Wolff P A 1954 *Phys. Rev.* **95** 1415
[2] Shockley W 1961 *Solid State Electron.* **2** 35
[3] Baraff G A 1962 *Phys. Rev.* **128** 2507
[4] Ridley B K 1983 *J. Phys. C: Solid State Phys.* **16** 3373, 4733
[5] Burt M G 1985 *J. Phys. C: Solid State Phys.* **18** L477
[6] Wilson S P 1994 *Solid-State Electron.* **37** 243
[7] Dumke W P 1968 *Phys. Rev.* **167** 783
[8] Quade W, Schöll E and Rudan M 1993 *Solid-State Electron.* **36** 1493
[9] Goldsman N, Wu Y J and Frey J 1990 *J. Appl. Phys.* **68** 1075
[10] Wang S L, Goldsman N and Hennacy K 1994 *J. Appl. Phys.* **71** 1815
[11] Wang Y and Brennan K F 1994 *J. Appl. Phys.* **75** 313, 974
[12] Oguzman I H, Wang Y, Kolnik J and Brennan K F 1995 *J. Appl. Phys.* **77** 225
[13] Keldysh L V 1965 *Zh. Exp. Teor. Fiz.* **48** 1962 (Engl. Transl. 1965 *Sov. Phys.–JETP* **21** 1135)
[14] Kunikiyo T, Takenaka M, Kamakura Y, Yamaji M, Mizuno H, Morifuji M, Taniguchi K and Hamaguchi C 1994 *J. Appl. Phys.* **75** 297
[15] Arnold D, Cartier E and DiMaria D J 1994 *Phys. Rev.* B **49** 10278
[16] Quade E, Schöll E, Rossi F and Jacoboni C 1994 *Phys. Rev.* **50** 7398
[17] Beattie A R and Landsberg P T 1959 *Proc. R. Soc.* A **249** 16
[18] Thoma R, Peifer H J, Engl W L, Quade W, Brunetti R and Jacoboni C 1991 *J. Appl. Phys.* **69** 2300
[19] Sano N and Yoshii A 1992 *Phys. Rev.* B **45** 4171
[20] Bude J and Hess K 1992 *J. Appl. Phys.* **72** 3554
[21] Martin M J, González T, Velázquez J E and Pardo D 1993 *Semicond. Sci. Technol.* **8** 1291
[22] Chandramouli V and Maziar C M 1993 *Solid-State Electron.* **36** 285
[23] Ershov M and Ryzhii V 1994 *J. Appl. Phys.* **76** 1672
[24] Yeom K, Hinchley J M and Singh J 1994 *Appl. Phys. Lett.* **64** 2985
[25] Bringuier E 1994 *Phys. Rev.* B **49** 7974
[26] Lei X L and Ting C S 1985 *Phys. Rev.* B **32** 1112
[27] Lei X L, Horing N J M and Cui H L 1991 *Phys. Rev. Lett.* **66** 3277
Lei X L 1992 *Phys. Status Solidi* b **170** 519
[28] Ridley B K 1988 *Quantum Processes in Semiconductors* 2nd edn (Oxford: Oxford University Press)
[29] Alberga G E, van Welzenis R G and de Zeeuw W C 1983 *Appl. Phys.* A **27** 107
[30] McGroddy J C and Nathan M I 1966 *J. Phys. Soc. Japan* **21** 437
[31] Toda M 1966 *J. Appl. Phys.* **37** 32